Table S1. Primer sequences for genotyping and qRT-PCR.

Primers for genotyping	Sequences
Angptl2-loxp-tF	ATCCTAATGTCCCTCTTGGC
Angptl2-FRT-tR	CAGGCTGTGAACAGGTTAGTCATC
Prx1-Cre-F	AGG GGG TCT GTA AAA CGT CA
Prx1-Cre-R	GTA CGG TCA GTA AAT TGG ACA CC
Pf4-Cre-F	CCCATACAGCACACCTTTTG
Pf4-Cre-R	TGCACAGTCAGCAGGTT
Cdh5-Cre-F	ATGTCCAATTTACTGACCGTACA
Cdh5-Cre-R	CGCATAACCAGTGAAACAGCATT
Tie2-Cre-F	ATTTGCCTGCATTACCGGTC
Tie2-Cre-R	ATCAACGTTTTCTTTTCGG

Primers for qRT-PCR	Sequences
Mouse-*Angptl2*-F	CCACCTCGGGTCTACCAAC
Mouse-*Angptl2*-R	CTTGCAGGCAGTCTCTCCAT
Mouse-*PPARd*-F	TTCAGAAATGCCTTGCAGTG
Mouse-*PPARd*-R	GGACTCTGGATTCAGCTGGT
Mouse-*Rora*-F	GTGGAGACAAATCGTCAGGAAT
Mouse-*Rora*-R	TGGTCCGATCAATCAAACAGTTC
Mouse-*Rab20*-F	GGGAGCAGTTTCATGGTCTGG
Mouse-*Rab20*-R	GCAGTCATTGTTGGCTGTTTC
Mouse-*Pik3r2*-F	GGATGCCTGGCTTCAACGA
Mouse-*Pik3r2*-R	CTGGGAGTATGTGGCCTGACT
Mouse-*Isg15*-F	GGTGTCCGTGACTAACTCCAT
Mouse-*Isg15*-R	TGGAAAGGGTAAGACCGTCCT
Mouse-*G0s2*-F	GTGCTCGGCCTAGTTGAGAC
Mouse-*G0s2*-R	CACCTGGGTCATGATCTGTG
Mouse-*CD49d*-F	GATGCTGTTGTTGTACTTCGGG
Mouse-*CD49d*-R	ACCACTGAGGCATTAGAGAGC
Mouse-*Egr1*-F	TCGGCTCCTTTCCTCACTCA
Mouse-*Egr1*-R	CTCATAGGGGTTGTTCGCTCGG
Mouse-*Mmp2*-F	CAAGTTCCCCGGCGATGTC
Mouse-*Mmp2*-R	TTCTGGTCAAGGTCACCTGTC
Mouse-*Mmp9*-F	CTGGACAGCCAGACACTAAAG
Mouse-*Mmp9*-R	CTCGCGGCAAGTCTTCAGAG

Table S2. The list of differentially expressed gene

GeneID	GeneName	Locus	CTRL_FPKM	A2_FPKM	log2(A2/CTRL)	up-or-down	p_value	q_value
ENSG00000271590	RP11-181E10.3	2:1111959	0.551329	0	-1.79769e+308	down	0.000119	0.003742
ENSG00000251660	AC007036.5	7:3013480	0.923752	0	-1.79769e+308	down	0.004509	0.047583
ENSG00000260583	AP000223.42	21:255827	0.726751	0	-1.79769e+308	down	0.004075	0.044865
ENSG00000226318	RPS3AP38	10:679218	1.1102	0	-1.79769e+308	down	0.000242	0.006469
ENSG00000261312	AC002550.5	16:195552	0.946634	0	-1.79769e+308	down	0.000139	0.004178
ENSG00000260570	RP11-24N18.1	16:288224	3.91865	0	-1.79769e+308	down	0.002153	0.029306
ENSG00000272498	RP11-415F23.3	3:1626515	0.855397	0	-1.79769e+308	down	0.002157	0.029306
ENSG00000188223	AC002398.9	19:357180	0.506095	0	-1.79769e+308	down	0.001617	0.024356
ENSG00000267343	ZNF833P	19:116397	0.790099	0	-1.79769e+308	down	4.09E-06	0.000302
ENSG00000283241	AC026348.1	3:1132110	0.499048	0	-1.79769e+308	down	1.29E-09	4.26E-07
ENSG00000270096	RP11-362K14.6	3:1697934	0.964971	0	-1.79769e+308	down	0.000889	0.016082
ENSG00000250309	CTC-345K18.2	5:1506608	1.13775	0	-1.79769e+308	down	0.00045	0.010212
ENSG00000254528	RP11-728F11.4	11:117427	0.504466	0	-1.79769e+308	down	0.004143	0.045324
ENSG00000267655	CTD-2286N8.2	18:790692	0.719614	0	-1.79769e+308	down	0.003619	0.04173
ENSG00000279415	RP11-1102P22.1	16:171017	0.930019	0	-1.79769e+308	down	8.81E-05	0.003052
ENSG00000256928	RP11-809N8.2	11:733762	1.73927	0	-1.79769e+308	down	8.20E-06	0.000505
ENSG00000259185	RP11-56B16.4	15:518296	2.15938	0	-1.79769e+308	down	0.000427	0.009859
ENSG00000254673	RP11-598P20.5	8:4284963	1.01374	0	-1.79769e+308	down	0.003436	0.040377
ENSG00000142511	GPR32	19:507704	0	0.613931	1.79769e+308	up	0.000266	0.006851
ENSG00000248919	ATP5J2-PTCD1	7:9932589	0	1.01094	1.79769e+308	up	9.13E-08	1.43E-05
ENSG00000228170	RP1-40E16.11	6:3118373	0	1.26287	1.79769e+308	up	0.001311	0.021007
ENSG00000260914	RP11-343C2.11	16:691055	0	4.60886	1.79769e+308	up	4.94E-12	4.28E-09
ENSG00000277957	SENP3-EIF4A1	17:756187	0	0.689481	1.79769e+308	up	5.16E-07	5.31E-05
ENSG00000273331	TM4SF19-TCTEX1D2	3:1962114	0	0.743669	1.79769e+308	up	0.004373	0.046848
ENSG00000266923	RP11-693J15.4	12:924200	0	0.589533	1.79769e+308	up	5.23E-05	0.002031
ENSG00000256249	RP11-324E6.6	12:122687	0	0.638206	1.79769e+308	up	0.000823	0.015137
ENSG00000107159	CA9	9:3565828	0	0.727885	1.79769e+308	up	0.000915	0.016349
ENSG00000185345	PARK2	6:1613474	0.0640323	2.06567	5.01166	up	1.05E-06	9.26E-05
ENSG00000123689	G0S2	1:2096613	0.115794	1.57297	3.76386	up	0.000147	0.00437
ENSG00000231475	IGHV4-31	14:106349	0.268864	2.44689	3.186	up	0.003235	0.038741
ENSG00000105697	HAMP	19:352807	0.165958	1.44134	3.11852	up	0.002082	0.028576
ENSG00000128656	CHN1	2:1747993	0.0862273	0.708295	3.03813	up	0.000301	0.007495
ENSG00000134827	TCN1	11:598527	0.20974	1.50854	2.84648	up	0.000121	0.003756
ENSG00000088827	SIGLEC1	20:368696	0.275743	1.72356	2.644	up	0	0
ENSG00000152467	ZSCAN1	19:580340	0.198722	1.21557	2.61281	up	0.000376	0.008965
ENSG00000163735	CXCL5	4:7399564	0.213851	1.28205	2.58378	up	1.46E-06	0.000123
ENSG00000105647	PIK3R2	19:181531	0.937232	5.56827	2.57075	up	1.38E-14	2.38E-11
ENSG00000124102	PI3	20:451748	0.440791	2.37423	2.42929	up	0.000644	0.01264
ENSG00000171657	GPR82	X:4151493	0.154171	0.816395	2.40473	up	0.002498	0.03225
ENSG00000277232	GTSE1-AS1	22:462951	0.26078	1.28606	2.30206	up	0.00093	0.016478
ENSG00000229413	RP11-274B21.12	7:1286536	0.724886	3.55371	2.2935	up	0.004227	0.046015
ENSG00000108691	CCL2	17:342552	6.35265	28.6042	2.1708	up	0	0
ENSG00000157601	MX1	21:414203	2.51541	11.0107	2.13004	up	0	0
ENSG00000283590	NDOR1	9:1372056	0.311921	1.32308	2.08465	up	0.000528	0.011284
ENSG00000014914	MTMR11	1:1499286	0.280052	1.1454	2.03209	up	0.001145	0.019055
ENSG00000262406	MMP12	11:102862	0.806775	3.1183	1.95052	up	1.68E-08	3.72E-06
ENSG00000254402	LRRC24	8:1445179	0.209151	0.726725	1.79687	up	0.002276	0.030429
ENSG00000100122	CRYBB1	22:265992	0.241642	0.837022	1.79239	up	0.004418	0.047098
ENSG00000275185	RP13-753N3.3	17:308973	1.36775	4.63736	1.7615	up	0.003103	0.037447
ENSG00000261459	AC002310.11	16:305240	0.45515	1.51789	1.73766	up	9.27E-05	0.003127
ENSG00000259112	NDUFC2-KCTD14	11:780157	3.39421	11.168	1.71823	up	1.70E-06	0.000139
ENSG00000267598	CTC-250I14.6	19:131504	1.15052	3.69481	1.68322	up	0.000619	0.012374
ENSG00000272540	XXbac-BPG252P9.9	6:3072020	1.45776	4.64034	1.67048	up	0.000477	0.010661
ENSG00000133424	LARGE1	22:331622	0.35596	1.12731	1.6631	up	0.001369	0.02175
ENSG00000250021	C15orf38-AP3S2	15:898305	0.89885	2.76817	1.62278	up	4.62E-05	0.001851
ENSG00000205927	OLIG2	21:329136	0.322656	0.98389	1.6085	up	7.24E-06	0.000473
ENSG00000137959	IFI44L	1:7861992	1.37449	4.16708	1.60015	up	7.13E-07	6.97E-05
ENSG00000225783	MIAT	22:266464	0.32039	0.969426	1.5973	up	1.15E-05	0.000668
ENSG00000105352	CEACAM4	19:416189	1.30371	3.93029	1.59202	up	5.10E-07	5.31E-05
ENSG00000274012	RN7SL2	14:498611	18.078	51.5685	1.51226	up	9.58E-11	5.51E-08
ENSG00000276085	CCL3L3	17:361832	1.84248	5.24933	1.51048	up	3.69E-07	4.25E-05
ENSG00000130589	HELZ2	20:635580	1.3346	3.6928	1.46831	up	1.35E-10	7.01E-08
ENSG00000163739	CXCL1	4:7386939	0.516566	1.39353	1.43172	up	0.004081	0.044877
ENSG00000131471	AOC3	17:428511	0.213279	0.573098	1.42604	up	0.004705	0.0488
ENSG00000257553	RP11-603J24.17	12:560798	2.51916	6.75633	1.4233	up	0.001572	0.02388
ENSG00000122035	RASL11A	13:272703	0.547983	1.45768	1.41147	up	0.003979	0.044085
ENSG00000139899	CBLN3	14:244265	0.361797	0.938307	1.37488	up	0.000517	0.011149
ENSG00000136689	IL1RN	2:1131072	25.41	64.5756	1.34559	up	0	0
ENSG00000260257	RP5-1085F17.3	20:328566	1.51331	3.84319	1.34459	up	7.75E-06	0.000495
ENSG00000111012	CYP27B1	12:577623	1.07949	2.74016	1.34392	up	0.000121	0.003756
ENSG00000161939	RNASEK-C17orf49	17:685386	2.16612	5.44244	1.32914	up	9.00E-05	0.00308

ENSG00000122641	INHBA	7:4166716	0.321298	0.794889	1.30684	up	8.87E-05	0.003056
ENSG00000129038	LOXL1	15:739080	0.997365	2.39421	1.26336	up	0.000101	0.003307
ENSG00000198483	ANKRD35	1:1458665	0.286955	0.68113	1.24711	up	0.000821	0.01513
ENSG00000158406	HIST1H4H	6:2627760	1.58014	3.73305	1.2403	up	0.002881	0.035519
ENSG00000173451	THAP2	12:716094	1.27078	2.98502	1.23203	up	0.000571	0.011804
ENSG00000231789	PIK3CD-AS2	1:9651731	0.912205	2.12224	1.21816	up	0.001988	0.027793
ENSG00000050730	TNIP3	4:1211314	0.894563	2.0606	1.20381	up	0.00012	0.003756
ENSG00000135119	RNFT2	12:116738	0.683773	1.56213	1.19192	up	0.001676	0.024961
ENSG00000280106	CTC-523E23.3	19:349490	1.40725	3.19563	1.18322	up	0.000398	0.009325
ENSG00000267757	EML2-AS1	19:456069	1.14246	2.57513	1.17251	up	0.004358	0.046763
ENSG00000126709	IFI6	1:2766606	16.7977	37.658	1.1647	up	1.76E-12	1.83E-09
ENSG00000187608	ISG15	1:1001137	11.352	25.3487	1.15897	up	1.89E-08	4.07E-06
ENSG00000186395	KRT10	17:408181	2.70924	6.00812	1.14903	up	1.05E-06	9.26E-05
ENSG00000275713	HIST1H2BH	6:2625165	0.809919	1.79021	1.14428	up	0.001132	0.018984
ENSG00000173926	3-Mar	5:1268677	1.76415	3.87937	1.13685	up	0.000279	0.007076
ENSG00000105699	LSR	19:352483	0.815273	1.75085	1.1027	up	0.003965	0.04402
ENSG00000110079	MS4A4A	11:602805	2.87826	6.08108	1.07913	up	1.94E-05	0.000975
ENSG00000185507	IRF7	11:612552	6.26489	13.2329	1.07877	up	1.02E-14	1.98E-11
ENSG00000279443	RP4-669K10.8	1:2854445	0.709833	1.47063	1.05088	up	0.003719	0.042379
ENSG00000139832	RAB20	13:110523	2.07201	4.2773	1.04567	up	3.68E-05	0.001533
ENSG00000102890	ELMO3	16:671991	0.990349	2.02478	1.03176	up	0.000324	0.008009
ENSG00000167680	SEMA6B	19:454259	0.512044	1.04589	1.0304	up	0.00027	0.006939
ENSG00000221955	SLC12A8	3:1250826	1.46141	2.97351	1.02481	up	5.80E-05	0.00219
ENSG00000222009	BTBD19	1:4480848	1.04788	2.09995	1.00288	up	0.00431	0.046617
ENSG00000150627	WDR17	4:1760658	3.95605	1.97721	-1.00059	down	5.83E-06	0.000396
ENSG00000215447	BX322557.10	21:452880	2.6021	1.29782	-1.00358	down	0.002488	0.032183
ENSG00000156011	PSD3	8:1852730	3.03748	1.51477	-1.00378	down	8.55E-05	0.002985
ENSG00000282827	ATRIP	3:4844670	5.25776	2.6128	-1.00885	down	7.09E-07	6.97E-05
ENSG00000205885	C1RL-AS1	12:708020	4.42729	2.14869	-1.04297	down	0.002415	0.031578
ENSG00000170006	TMEM154	4:1526186	4.44741	2.11452	-1.07263	down	6.25E-05	0.002322
ENSG00000133138	TBC1D8B	X:1068026	1.79942	0.849793	-1.08235	down	0.000562	0.011652
ENSG00000154874	CCDC144B	17:185112	3.19356	1.46857	-1.12076	down	0.000212	0.005892
ENSG00000213865	C8orf44	8:6666759	3.27189	1.49996	-1.1252	down	0.000747	0.01406
ENSG00000258461	RP11-164J13.1	15:422084	1.82498	0.832976	-1.13153	down	2.49E-05	0.001155
ENSG00000278811	LINC00624	1:1471727	0.936222	0.426252	-1.13514	down	0.002088	0.028595
ENSG00000163625	WDFY3	4:8466960	5.58145	2.53212	-1.1403	down	9.35E-08	1.44E-05
ENSG00000144935	TRPC1	3:1427240	1.67021	0.755465	-1.1446	down	0.004573	0.048008
ENSG00000261684	RP11-265N6.1	15:424912	6.41714	2.87445	-1.15865	down	0.003882	0.043634
ENSG00000224186	C5orf66	5:1350277	4.84448	2.16723	-1.16049	down	1.63E-05	0.000877
ENSG00000182389	CACNB4	2:1517889	0.948596	0.421918	-1.16883	down	0.001967	0.027628
ENSG00000280046	RP11-1099M24.6	17:785668	1.93125	0.854651	-1.17613	down	9.86E-06	0.000594
ENSG00000272760	RP11-5C23.1	7:1549284	3.02926	1.32563	-1.19229	down	0.003839	0.043202
ENSG00000134297	PLEKHA8P1	12:451730	3.8208	1.65302	-1.20877	down	0.002379	0.031389
ENSG00000070087	PFN2	3:1497611	1.60886	0.693904	-1.21323	down	0.002629	0.033394
ENSG00000145075	CCDC39	3:1806021	0.931952	0.400456	-1.21861	down	0.000258	0.006757
ENSG00000258559	AC005519.4	14:742854	1.97859	0.845551	-1.22651	down	0.002652	0.033498
ENSG00000148483	TMEM236	10:177522	0.510558	0.216766	-1.23594	down	0.003314	0.039411
ENSG00000249087	ZNF436-AS1	1:2335944	0.826194	0.344482	-1.26205	down	0.003127	0.037636
ENSG00000122254	HS3ST2	16:228141	0.825039	0.34363	-1.26361	down	0.00188	0.026767
ENSG00000187554	TLR5	1:2231094	1.17664	0.489511	-1.26527	down	0.000558	0.011593
ENSG00000157429	ZNF19	16:714475	1.17282	0.478933	-1.29208	down	0.003001	0.03668
ENSG00000279767	AL513523.2	1:1537280	5.55705	2.14665	-1.37223	down	0.000133	0.004061
ENSG00000165115	KIF27	9:8382965	2.49388	0.949272	-1.3935	down	5.51E-07	5.59E-05
ENSG00000230590	FTX	X:7394432	3.3519	1.25847	-1.4133	down	0.001017	0.017494
ENSG00000147231	CXorf57	X:1066119	1.25274	0.469986	-1.4144	down	0.002967	0.036286
ENSG00000149054	ZNF215	11:682194	1.1653	0.434366	-1.42372	down	0.00433	0.046645
ENSG00000179240	RP11-111M22.2	11:763813	2.79909	1.0383	-1.43073	down	1.23E-05	0.000708
ENSG00000069667	RORA	15:604791	1.59953	0.588331	-1.44295	down	4.86E-06	0.000344
ENSG00000189144	ZNF573	19:377358	2.47291	0.891586	-1.47176	down	0.002841	0.035227
ENSG00000100154	TTC28	22:278516	3.46701	1.19254	-1.53965	down	3.82E-10	1.48E-07
ENSG00000009694	TENM1	X:1239592	0.681777	0.231028	-1.56123	down	0.002572	0.032927
ENSG00000279576	AP000769.1	11:654977	5.93931	1.9336	-1.61901	down	4.00E-05	0.001651
ENSG00000272367	CTC-428H11.2	5:8726788	2.62421	0.843928	-1.63669	down	0.004275	0.046335
ENSG00000155962	CLIC2	X:1552762	1.05847	0.33902	-1.64253	down	0.000647	0.012652
ENSG00000163464	CXCR1	2:2181628	0.616076	0.190665	-1.69207	down	0.003534	0.041093
ENSG00000283467	AL078584.1	6:2479732	1.35349	0.406129	-1.73668	down	0.001235	0.020219
ENSG00000259205	PRKXP1	15:100553	1.29425	0.387793	-1.73876	down	0.002063	0.028465
ENSG00000279192	PWAR5	15:248236	2.14662	0.627427	-1.77455	down	5.10E-07	5.31E-05
ENSG00000174501	ANKRD36C	2:9583691	7.21993	2.09447	-1.7854	down	6.81E-12	5.03E-09
ENSG00000215158	RP11-1023L17.1	5:3416469	6.49359	1.87627	-1.79115	down	2.26E-07	2.79E-05
ENSG00000215630	GUSBP9	5:7119764	2.45158	0.682042	-1.84578	down	0.004538	0.047821
ENSG00000184566	RP13-786C16.1	11:338585	1.43556	0.388511	-1.88558	down	0.003452	0.040501

ENSG00000279500	RP11-21K12.2	12:128793	1.42718	0.368813	-1.9522	down	0.000508	0.011003
ENSG00000281195	ZNF638-IT1	2:7127656	1.17209	0.295956	-1.98563	down	0.004337	0.046648
ENSG00000196876	SCN8A	12:515902	0.816187	0.199038	-2.03585	down	0.000922	0.01639
ENSG00000279390	AF127577.13	21:148188	1.40601	0.336626	-2.06239	down	5.09E-05	0.001981
ENSG00000156113	KCNMA1	10:768696	0.620525	0.144481	-2.10261	down	0.000856	0.015632
ENSG00000279456	RP11-87H9.5	9:4099224	1.2326	0.285048	-2.11242	down	0.000789	0.014676
ENSG00000279041	CTD-2373N4.3	8:3038211	0.937683	0.199048	-2.23598	down	0.002877	0.035495
ENSG00000213240	RP11-458D21.5	1:1460646	0.49666	0.099484	-2.31972	down	0.002616	0.033282
ENSG00000279530	AC092881.1	12:697386	0.941205	0.186367	-2.33636	down	0.000636	0.012555
ENSG00000261604	CTD-2636A23.2	5:4328760	1.4528	0.255767	-2.50594	down	5.25E-05	0.002034
ENSG00000214262	ANKRD36BP1	1:1682259	2.09186	0.326527	-2.67951	down	0.00039	0.009172
ENSG00000251201	TMED7-TICAM2	5:1155786	0.92002	0.136447	-2.75333	down	0.000224	0.006101
ENSG00000261366	MANEA-AS1	6:9557518	1.05895	0.154407	-2.77783	down	0.000313	0.007754
ENSG00000247228	RP11-296I10.3	16:701136	1.58993	0.197523	-3.00887	down	3.32E-05	0.001425
ENSG00000229267	AC072062.1	2:2148102	0.816714	0.100704	-3.01971	down	0.002479	0.032116
ENSG00000267500	ZNF887P	19:116397	1.07164	0.115972	-3.20797	down	0.001467	0.022757
ENSG00000259024	TVP23C-CDRT4	17:154360	1.18964	0.121987	-3.28572	down	0.004808	0.049586
ENSG00000177675	CD163L1	12:734668	0.650257	0.060022	-3.43745	down	0.001514	0.023306
ENSG00000176927	EFCAB5	17:295605	0.560929	0.047427	-3.56403	down	0.00064	0.012593
ENSG00000143248	RGS5	1:1631111	0.736425	0.059732	-3.62397	down	3.33E-05	0.001425
ENSG00000261845	RP13-638C3.4	17:825197	1.38393	0.099812	-3.79342	down	0.004841	0.049794
ENSG00000257411	RP11-603J24.9	12:560798	5.36556	0.342108	-3.97121	down	0.002784	0.034735
ENSG00000232104	RFX3-AS1	9:3526722	1.14708	0.054351	-4.39952	down	0.003353	0.039789
ENSG00000103888	CEMIP	15:807793	0.598823	0.026877	-4.47771	down	0.000157	0.004619

Table S3. The list of pathway enrichment analysis

| #Pathway	Sample1 (49)	Sample2 (12412)	Pvalue	Qvalue	Pathway ID	Genes	KOs
Chemokine signaling pathway	5	178	0.00066	0.06233	ko04062	ENSG00000105647;ENSG00000163739;ENSG00000163735;ENSG00000163464;ENSG00000108691	K02649+K05505+K05506+K04175+K14624
Cytokine-cytokine receptor interaction	5	263	0.00366	0.13891	ko04060	ENSG00000122641;ENSG00000163739;ENSG00000163735;ENSG00000163464;ENSG00000108691	K04667+K05505+K05506+K04175+K14624
Rheumatoid arthritis	3	91	0.00551	0.13891	ko05323	ENSG00000163739;ENSG00000163735;ENSG00000108691	K05505+K05506+K14624
Salmonella infection	3	93	0.00585	0.13891	ko05132	ENSG00000187554;ENSG00000163739;ENSG00000070087	K10168+K05505+K05759
Pancreatic secretion	3	107	0.00861	0.16356	ko04972	ENSG00000144935;ENSG00000156113;ENSG00000107159	K04964+K04936+K01672
Legionellosis	2	58	0.02193	0.29761	ko05134	ENSG00000187554;ENSG00000163739	K10168+K05505
NOD-like receptor signaling pathway	2	58	0.02193	0.29761	ko04621	ENSG00000163739;ENSG00000108691	K05505+K14624
Epithelial cell signaling in Helicobacter pylori infection	2	70	0.0311	0.32894	ko05120	ENSG00000163739;ENSG00000163464	K05505+K04175
Influenza A	3	174	0.03116	0.32894	ko05164	ENSG00000157601;ENSG00000105647;ENSG00000108691	K14754+K02649+K14624
Pathogenic Escherichia coli infection	2	101	0.06023	0.43555	ko05130	ENSG00000186395;ENSG00000187554	K07604+K10168
Amoebiasis	2	103	0.06234	0.43555	ko05146	ENSG00000105647;ENSG00000163739	K02649+K05505
Chagas disease (American trypanosomiasis)	2	104	0.06341	0.43555	ko05142	ENSG00000105647;ENSG00000108691	K02649+K14624
Toll-like receptor signaling pathway	2	105	0.06448	0.43555	ko04620	ENSG00000105647;ENSG00000187554	K02649+K10168
Phenylalanine metabolism	1	18	0.06877	0.43555	ko00360	ENSG00000131471	K00276
Steroid biosynthesis	1	18	0.06877	0.43555	ko00100	ENSG00000111012	K07438
Parkinson's disease	2	118	0.07896	0.45917	ko05012	ENSG00000259112;ENSG00000185345	K03968+K04556
Circadian rhythm - mammal	1	22	0.08341	0.45917	ko04710	ENSG00000069667	K08532
Measles	2	133	0.09679	0.45917	ko05162	ENSG00000157601;ENSG00000105647	K14754+K02649
Glycosaminoglycan biosynthesis - heparan sulfate	1	26	0.09783	0.45917	ko00534	ENSG00000122254	K07808
Systemic lupus erythematosus	2	135	0.09925	0.45917	ko05322	ENSG00000158406;ENSG00000275713	K11254+K11252
beta-Alanine metabolism	1	31	0.11554	0.45917	ko00410	ENSG00000131471	K00276
Proximal tubule bicarbonate reclamation	1	32	0.11904	0.45917	ko04964	ENSG00000107159	K01672
Tyrosine metabolism	1	37	0.13634	0.45917	ko00350	ENSG00000131471	K00276
Collecting duct acid secretion	1	37	0.13634	0.45917	ko04966	ENSG00000107159	K01672
Aldosterone-regulated sodium reabsorption	1	37	0.13634	0.45917	ko04960	ENSG00000105647	K02649
Glycine, serine and threonine metabolism	1	37	0.13634	0.45917	ko00260	ENSG00000131471	K00276
Alcoholism	2	179	0.15715	0.45917	ko05034	ENSG00000158406;ENSG00000275713	K11254+K11252
Type II diabetes mellitus	1	45	0.16332	0.45917	ko04930	ENSG00000105647	K02649
Malaria	1	47	0.16994	0.45917	ko05144	ENSG00000108691	K14624
mTOR signaling pathway	1	49	0.17651	0.45917	ko04150	ENSG00000105647	K02649
Carbohydrate digestion and absorption	1	50	0.17977	0.45917	ko04973	ENSG00000105647	K02649
Fanconi anemia pathway	1	50	0.17977	0.45917	ko03460	ENSG00000282827	K10905
Non-small cell lung cancer	1	51	0.18302	0.45917	ko05223	ENSG00000105647	K02649
Endocytosis	2	199	0.18525	0.45917	ko04144	ENSG00000156011;ENSG00000163464	K12494+K04175
Endometrial cancer	1	52	0.18626	0.45917	ko05213	ENSG00000105647	K02649
Acute myeloid leukemia	1	58	0.20543	0.45917	ko05221	ENSG00000105647	K02649
Glioma	1	58	0.20543	0.45917	ko05214	ENSG00000105647	K02649
Regulation of actin cytoskeleton	2	216	0.20967	0.45917	ko04810	ENSG00000105647;ENSG00000070087	K02649+K05759
Colorectal cancer	1	62	0.21796	0.45917	ko05210	ENSG00000105647	K02649
VEGF signaling pathway	1	63	0.22107	0.45917	ko04370	ENSG00000105647	K02649
Bacterial invasion of epithelial cells	1	66	0.2303	0.45917	ko05100	ENSG00000105647	K02649
Melanoma	1	67	0.23336	0.45917	ko05218	ENSG00000105647	K02649
Pancreatic cancer	1	67	0.23336	0.45917	ko05212	ENSG00000105647	K02649
Renal cell carcinoma	1	68	0.2364	0.45917	ko05211	ENSG00000105647	K02649
Shigellosis	1	68	0.2364	0.45917	ko05131	ENSG00000070087	K05759
RIG-I-like receptor signaling pathway	1	70	0.24245	0.45917	ko04622	ENSG00000187608	K12159
Chronic myeloid leukemia	1	70	0.24245	0.45917	ko05220	ENSG00000105647	K02649
Fc epsilon RI signaling pathway	1	72	0.24845	0.45917	ko04664	ENSG00000105647	K02649
TGF-beta signaling pathway	1	73	0.25144	0.45917	ko04350	ENSG00000122641	K04667
Pertussis	1	75	0.25737	0.45917	ko05133	ENSG00000163735	K05506
Arrhythmogenic right ventricular cardiomyopathy (ARVC)	1	79	0.2691	0.45917	ko05412	ENSG00000182389	K04865
Phosphatidylinositol signaling system	1	80	0.27201	0.45917	ko04070	ENSG00000105647	K02649
Staphylococcus aureus infection	1	81	0.2749	0.45917	ko05150	ENSG00000186395	K07604
ErbB signaling pathway	1	82	0.27778	0.45917	ko04012	ENSG00000105647	K02649
Gastric acid secretion	1	83	0.28065	0.45917	ko04971	ENSG00000107159	K01672
B cell receptor signaling pathway	1	83	0.28065	0.45917	ko04662	ENSG00000105647	K02649
Small cell lung cancer	1	85	0.28636	0.45917	ko05222	ENSG00000105647	K02649
Apoptosis	1	85	0.28636	0.45917	ko04210	ENSG00000105647	K02649
Salivary secretion	1	87	0.29202	0.45917	ko04970	ENSG00000156113	K04936
Progesterone-mediated oocyte maturation	1	88	0.29483	0.45917	ko04914	ENSG00000105647	K02649
Cardiac muscle contraction	1	88	0.29483	0.45917	ko04260	ENSG00000182389	K04865
NF-kappa B signaling pathway	1	97	0.31968	0.47118	ko04064	ENSG00000163739	K05505
Fc gamma R-mediated phagocytosis	1	97	0.31968	0.47118	ko04666	ENSG00000105647	K02649
Hypertrophic cardiomyopathy (HCM)	1	98	0.32238	0.47118	ko05410	ENSG00000182389	K04865
Bile secretion	1	98	0.32238	0.47118	ko04976	ENSG00000107159	K01672
T cell receptor signaling pathway	1	104	0.33841	0.47588	ko04660	ENSG00000105647	K02649
Dilated cardiomyopathy	1	104	0.33841	0.47588	ko05414	ENSG00000182389	K04865
Prostate cancer	1	105	0.34104	0.47588	ko05215	ENSG00000105647	K02649
Cholinergic synapse	1	109	0.35147	0.47588	ko04725	ENSG00000105647	K02649
Vascular smooth muscle contraction	1	114	0.36429	0.47588	ko04270	ENSG00000156113	K04936
Leukocyte transendothelial migration	1	114	0.36429	0.47588	ko04670	ENSG00000105647	K02649
Glutamatergic synapse	1	115	0.36682	0.47588	ko04724	ENSG00000144935	K04964
Serotonergic synapse	1	117	0.37186	0.47588	ko04726	ENSG00000144935	K04964
Neurotrophin signaling pathway	1	117	0.37186	0.47588	ko04722	ENSG00000105647	K02649
Oxidative phosphorylation	1	120	0.37934	0.47588	ko00190	ENSG00000259112	K03968
Axon guidance	1	122	0.38428	0.47588	ko04360	ENSG00000167680	K06842
Toxoplasmosis	1	129	0.40126	0.47588	ko05145	ENSG00000105647	K02649
Osteoclast differentiation	1	129	0.40126	0.47588	ko04380	ENSG00000105647	K02649
Hepatitis C	1	130	0.40365	0.47588	ko05160	ENSG00000105647	K02649
Cell adhesion molecules (CAMs)	1	132	0.4084	0.47588	ko04514	ENSG00000088827	K06548
Natural killer cell mediated cytotoxicity	1	132	0.4084	0.47588	ko04650	ENSG00000105647	K02649
Insulin signaling pathway	1	133	0.41076	0.47588	ko04910	ENSG00000105647	K02649
Ubiquitin mediated proteolysis	1	137	0.42011	0.48085	ko04120	ENSG00000185345	K04556
Jak-STAT signaling pathway	1	156	0.46258	0.52315	ko04630	ENSG00000105647	K02649
Alzheimer's disease	1	162	0.47534	0.52971	ko05010	ENSG00000259112	K03968
Protein processing in endoplasmic reticulum	1	164	0.47953	0.52971	ko04141	ENSG00000185345	K04556
Tuberculosis	1	176	0.50399	0.55033	ko05152	ENSG00000111012	K07438
Herpes simplex infection	1	183	0.51773	0.55891	ko05168	ENSG00000108691	K14624
Focal adhesion	1	187	0.52541	0.56083	ko04510	ENSG00000105647	K02649
Huntington's disease	1	193	0.53671	0.56418	ko05016	ENSG00000259112	K03968
Epstein-Barr virus infection	1	195	0.54042	0.56418	ko05169	ENSG00000105647	K02649
MAPK signaling pathway	1	247	0.62726	0.64771	ko04010	ENSG00000182389	K04865
HTLV-I infection	1	255	0.6391	0.65285	ko05166	ENSG00000105647	K02649
Pathways in cancer	1	337	0.74114	0.74902	ko05200	ENSG00000105647	K02649
Metabolic pathways	3	1125	0.83351	0.83351	ko01100	ENSG00000259112;ENSG00000131471;ENSG00000111012	K03968+K00276+K07438

Figure S1
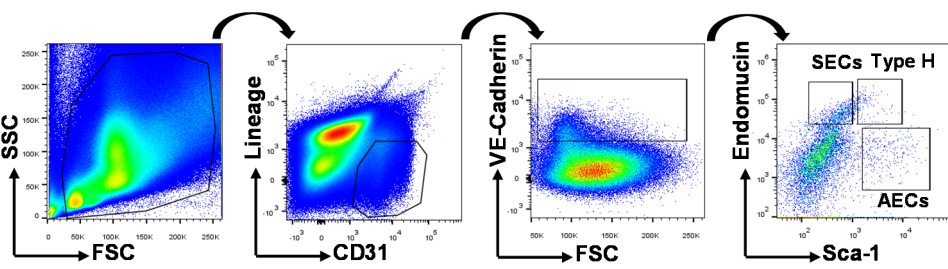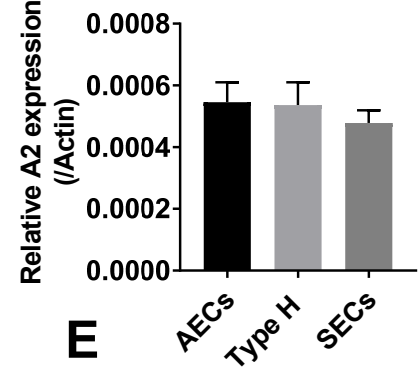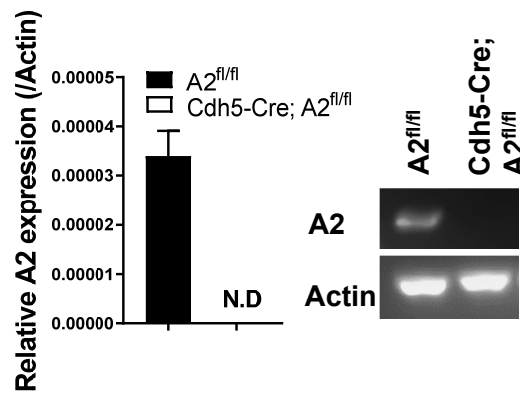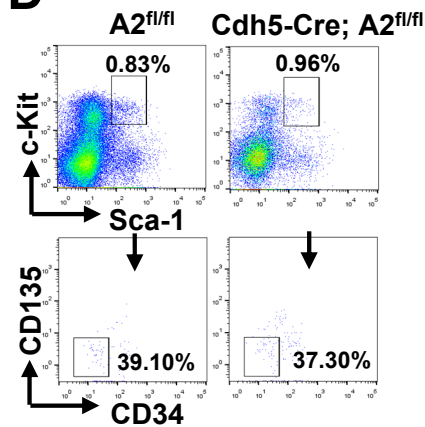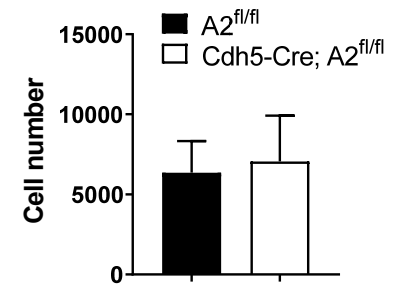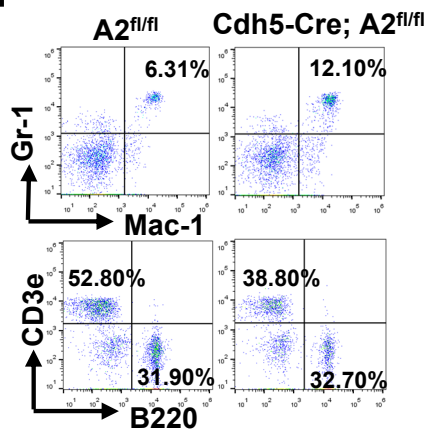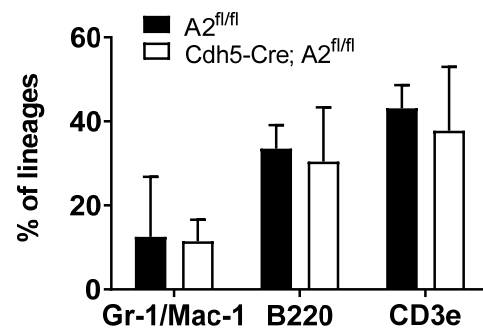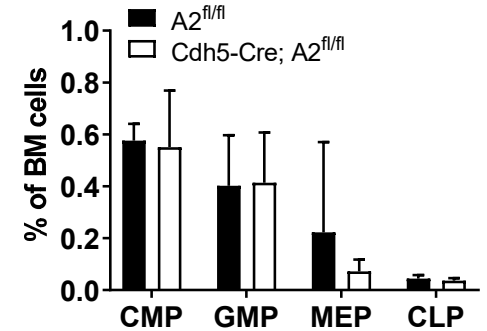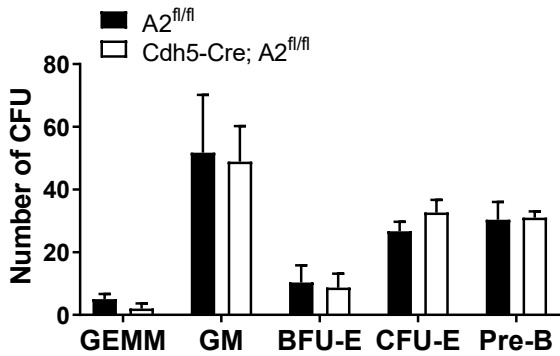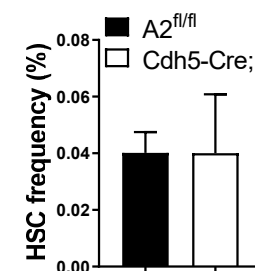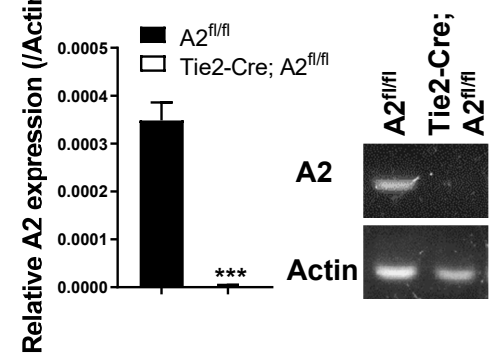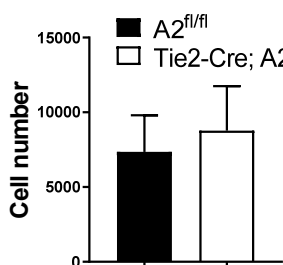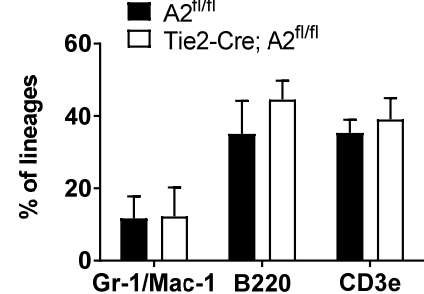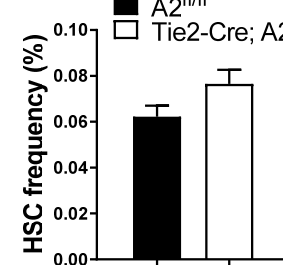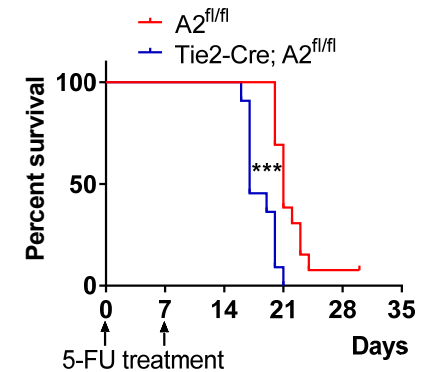
Figure S1, related to Figure 1. ANGPTL2 is highly expressed in endothelial cells and important for HSC stemness maintenance. (A) The flow cytometric sorting strategy for the indicated endothelial cell subtypes in BM, including sinusoidal ECs (SECs, Lin⁻CD31⁺VE-cad⁺EMCN⁺Sca1^{lo}), type H vessels (Lin⁻CD31⁺VE-cad⁺EMCN^{hi}Sca1⁺) and arterioles (Lin⁻CD31⁺VE-cad⁺EMCN⁻Sca1⁺). (B) The *Angptl2* mRNA expression level in the subtypes of the endothelial cells in BM. (C) The deletion efficiency of *Angptl2* in endothelial cells from *Cdh5-Cre; Angptl2$^{fl/fl}$* mice was measured by quantitative RT-PCR (left, n=3; ND, not detectable), and a representative electrophoretic image is shown (right). (D) Representative flow cytometric analyses of the frequencies of immunophenotypic Lin⁻Sca-1⁺c-Kit⁺CD34⁻CD135⁻ LT-HSCs from *Angptl2$^{fl/fl}$* and *Cdh5-Cre; Angptl2$^{fl/fl}$* mice. (E) The absolute number of LT-HSCs in BM in *Cdh5-Cre; Angptl2$^{fl/fl}$* and *Angptl2$^{fl/fl}$* control mice. (F-G) Representative flow cytometric analyses and quantification data of the multilineage cells in peripheral blood from *Angptl2$^{fl/fl}$* and *Cdh5-Cre; Angptl2$^{fl/fl}$* mice (n=3). (H) The cell frequencies of common myeloid progenitors (CMPs), granulocyte-monocyte progenitors (GMPs), megakaryocyte-erythroid progenitors (MEPs) and lymphoid progenitors (CLPs) in the BM of *Angptl2$^{fl/fl}$* and *Cdh5-Cre; Angptl2$^{fl/fl}$* mice (n=5). (I) The colony forming abilities were measured with total BM cells from *Angptl2$^{fl/fl}$* and *Cdh5-Cre; Angptl2$^{fl/fl}$* mice, and the colony numbers of CFU-GEMM, CFU-GM, BFU-E, CFU-E and pre-B colonies are shown (n=3~9). (J) The frequencies of LT-HSCs in *Angptl2$^{fl/fl}$* or *Cdh5-Cre; Angptl2$^{fl/fl}$* recipient mice receiving CD45.1 BM cells 6 months after transplantation. (K) The deletion efficiency of *Angptl2* in endothelial cells from *Tie2-Cre; Angptl2$^{fl/fl}$* mice was measured by quantitative RT-PCR (left, n=3), and a representative electrophoretic image is shown (right). (L) The absolute number of HSCs in BM in *Tie2-Cre; Angptl2$^{fl/fl}$* and *Angptl2$^{fl/fl}$* control mice. (M) Quantification data of the multilineage cells in peripheral blood from *Angptl2$^{fl/fl}$* and *Tie2-Cre; Angptl2$^{fl/fl}$* mice (n=3) (***$p < 0.001$). (N) The frequencies of LT-HSCs in *Angptl2$^{fl/fl}$* or *Tie2-Cre; Angptl2$^{fl/fl}$* recipient mice receiving CD45.1 BM cells 6 months after transplantation. (O) *Angptl2$^{fl/fl}$* and *Tie2-Cre; Angptl2$^{fl/fl}$* mice were treated with 5-FU and overall survival was analyzed (n=8, log-rank test, ***$p < 0.001$).

Figure S2
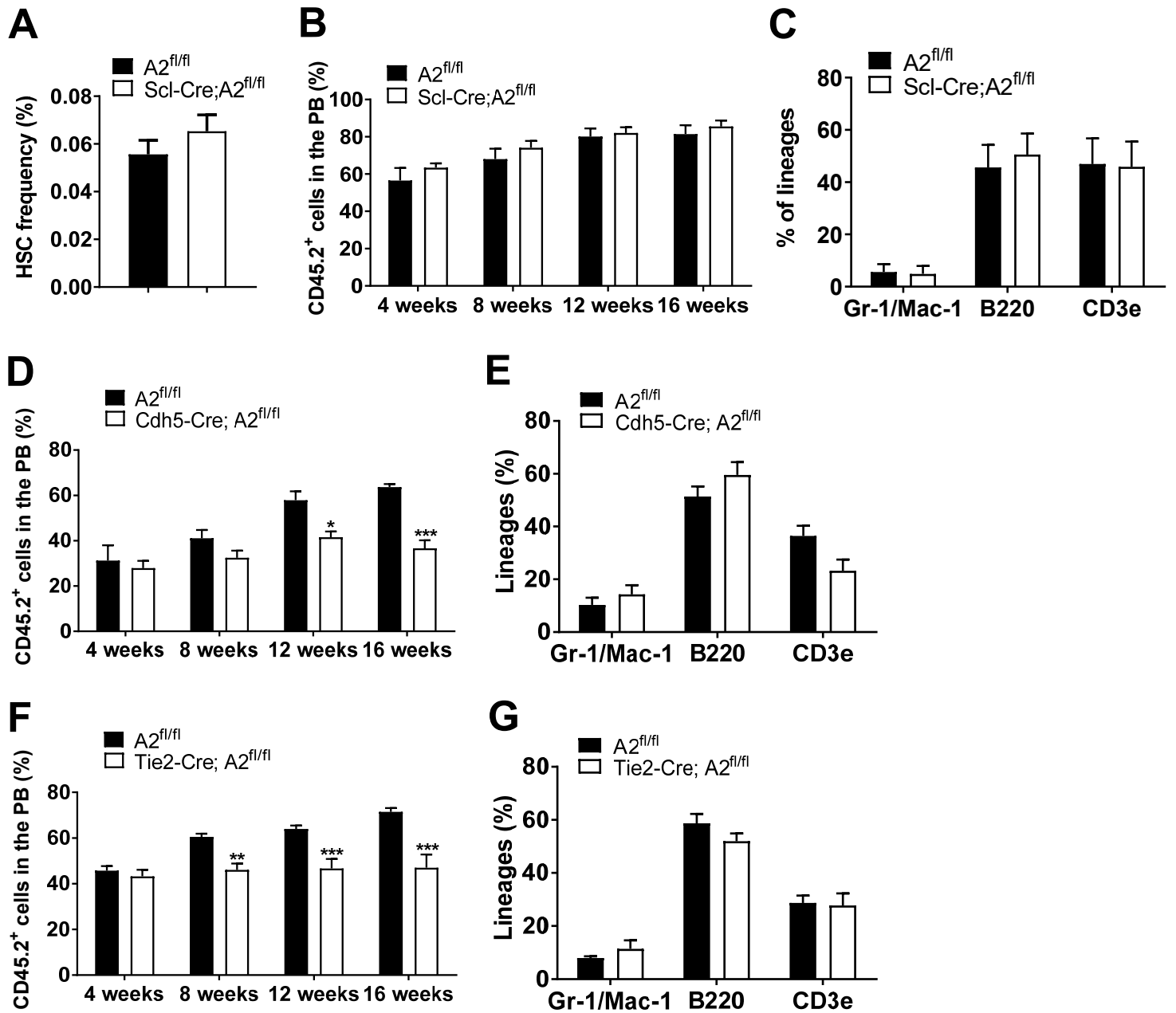
Figure S2, related to Figure 2. ANGPTL2 derived from other niche cells or HSCs has no effect on HSC activities. (A) The frequencies of LT-HSCs in *Angptl2$^{fl/fl}$* and *SCL-Cre-ERT; Angptl2$^{fl/fl}$* mice was determined 3 weeks after tamoxifen treatment (n=3). (B) BM CD45.2 cells from *Angptl2$^{fl/fl}$* or *SCL-Cre-ERT; Angptl2$^{fl/fl}$* (pretreated with tamoxifen for 3 weeks) along with CD45.1 competitor cells were injected into lethally irradiated CD45.1 recipient mice. Repopulation was analyzed at 4, 8, 12 and 16 weeks after transplantation (n=5). (C) Multilineage contribution of donor cells in the primary recipients in panel B) at 16 weeks post-transplantation (n=5). (D-G) The repopulation abilities of donor LT-HSCs isolated from *Angptl2$^{fl/fl}$*, *Cdh5-Cre; Angptl2$^{fl/fl}$* (D) or *Tie2-Cre; Angptl2$^{fl/fl}$* (F) mice was determined by flow cytometric analyses at the indicated time points. The multilineage contribution of donor cells in peripheral blood was quantified at 16 weeks after transplantation (E and G, n=5). (*$p <$ 0.05; **$p <$ 0.01; ***$p <$ 0.001).
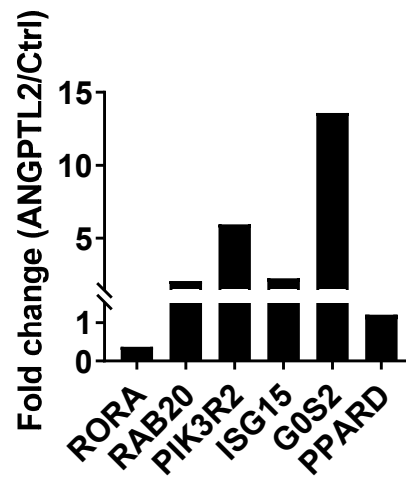
Figure S3
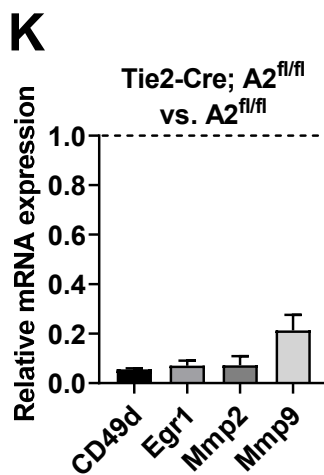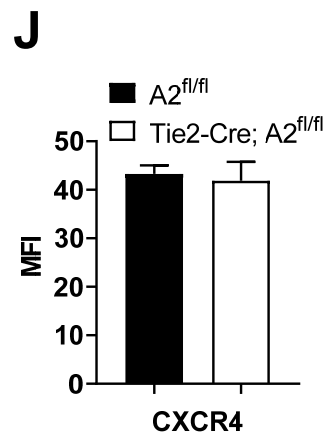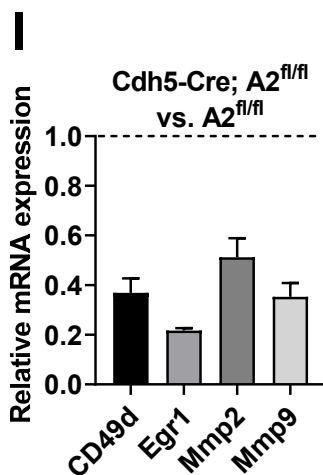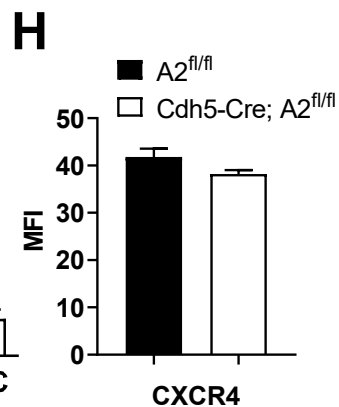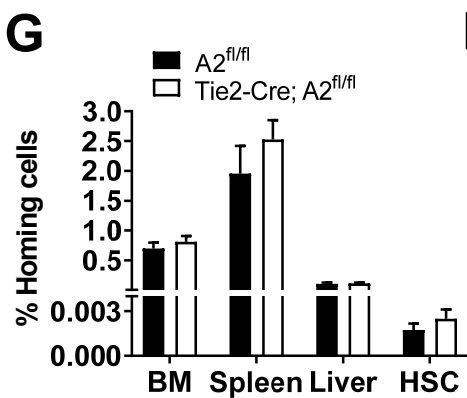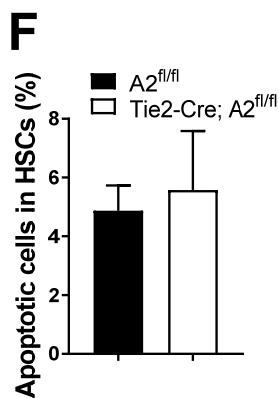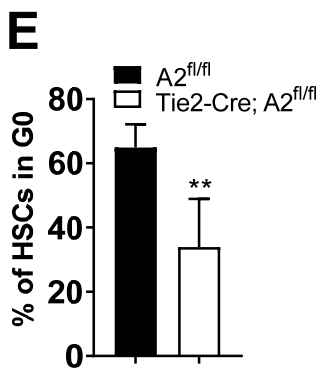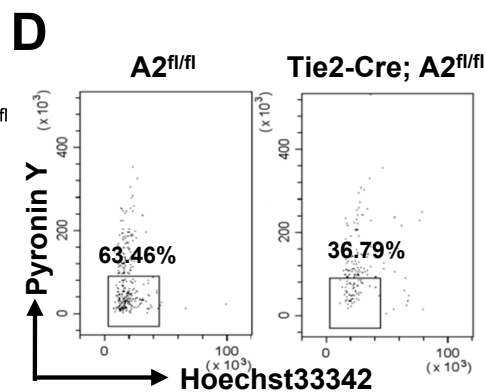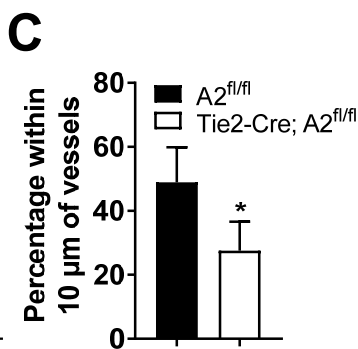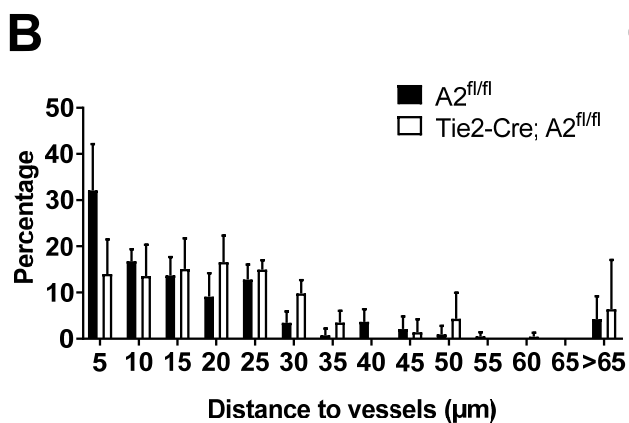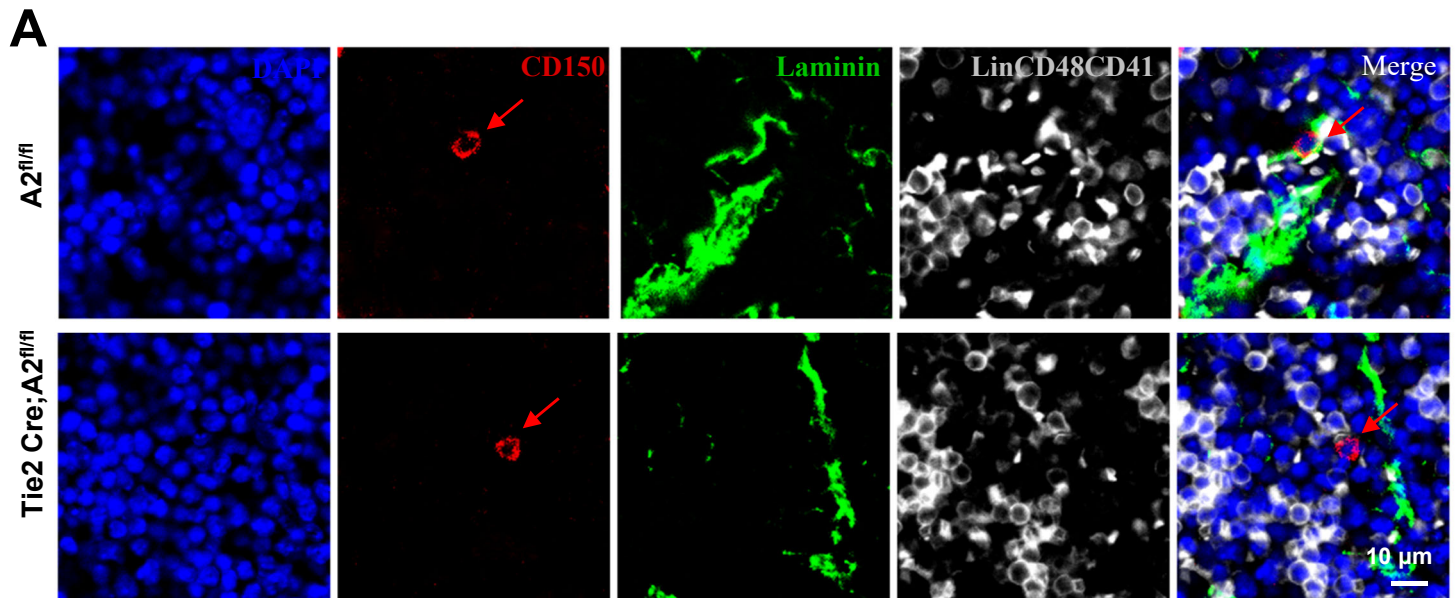
Figure S3, related to Figure 3. ANGPTL2-producing endothelium supports the localization of HSCs in BM niches. (A) Representative images of the localization of LT-HSCs in the BM of *Angptl2^{fl/fl}* or *Tie2-Cre; Angptl2^{fl/fl}* mice. BM sections were stained to reveal Lin^-CD150^+CD48^-CD41^- LT-HSCs (red, with arrowhead), laminin^+ vessels (green) and Lin^+CD41^+CD48^+ differentiated hematopoietic cells (gray). Scale bar, 10 μm. (B) Quantification of the frequencies of LT-HSCs localized at the indicated distance to vessels. n=134~142 cells/group. (C) The percentages of LT-HSCs in the BM of *Angptl2^{fl/fl}* and *Tie2-Cre2; Angptl^{fl/fl}* mice adjacent to laminin^+ endothelial cells (within 10 μm) are shown. A total of 134~142 LT-HSCs were counted (n=4). (D-E) The cell cycle status of LT-HSCs from *Angptl2^{fl/fl}* and *Tie2-Cre; Angptl2^{fl/fl}* mice was determined by staining with Hoechst 33342 and pyronin Y (D). The percentages of the G0 fraction in panel D are shown in E (n=4). (F) The apoptotic status of LT-HSCs from *Angptl2^{fl/fl}* or *Tie2-Cre; Angptl2^{fl/fl}* mice was measured by using Annexin V and 7-AAD staining (n=4). (G) BM cells from *Angptl2^{fl/fl}* and *Tie2-Cre; Angptl2^{fl/fl}* mice were labeled with CFSE and transplanted into lethally irradiated recipient mice. The percentage of CFSE^+ cells in the BM, spleen and liver or CFSE^+ LSK cells in the BM was determined by flow cytometric analysis 16 hr later (n=5). (H) The CXCR4 protein levels in LT-HSCs purified from *Angptl2^{fl/f}* or *Cdh5-Cre; Angptl2^{fl/fl}* was confirmed by flow cytometric analysis (n=3). (I) The mRNA expression levels of *CD49d*, *Egr1*, *Mmp2*, *Mmp9* in LT-HSCs isolated from *Angptl2^{fl/f}* or *Cdh5-Cre; Angptl2^{fl/fl}* were determined by quantitative RT-PCR (n=3). (J) The CXCR4 protein levels in LT-HSCs purified from *Angptl2^{fl/f}* or *Tie2-Cre; Angptl2^{fl/fl}* was confirmed by flow cytometric analysis (n=3). (K) The mRNA expression levels of *CD49d*, *Egr1*, *Mmp2*, *Mmp9* in LT-HSCs isolated from *Angptl2^{fl/f}* or *Tie2-Cre; Angptl2^{fl/fl}* were determined by quantitative RT-PCR (n=3). (*$p < 0.05$; **$p < 0.01$).
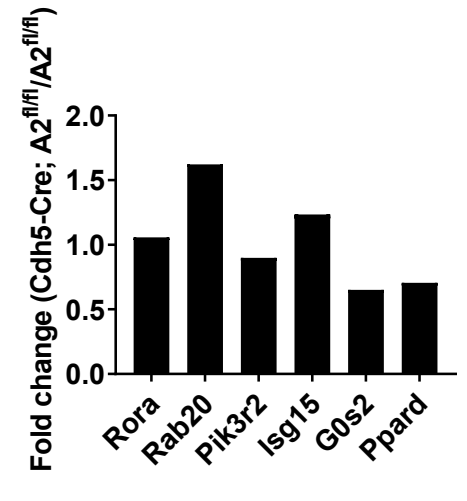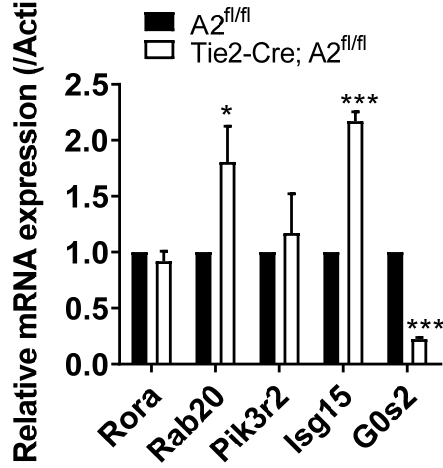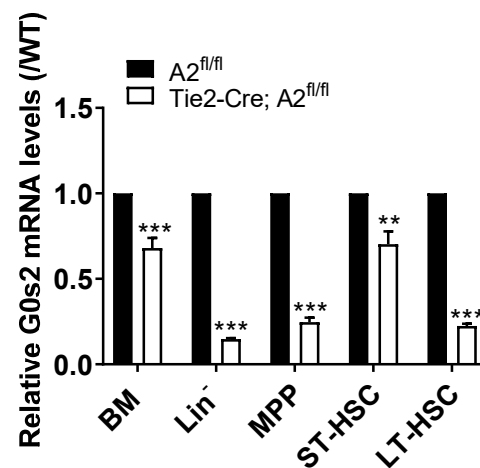
Figure S4
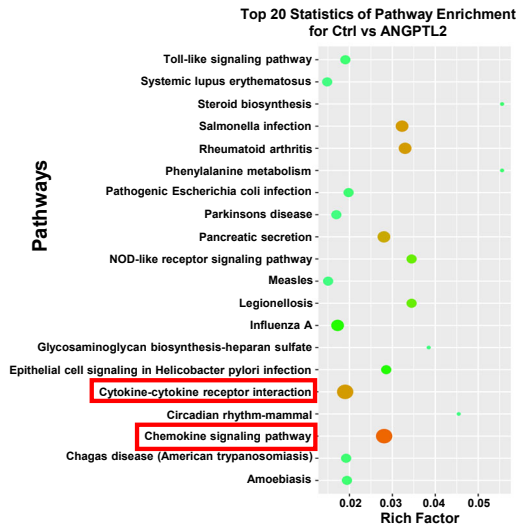
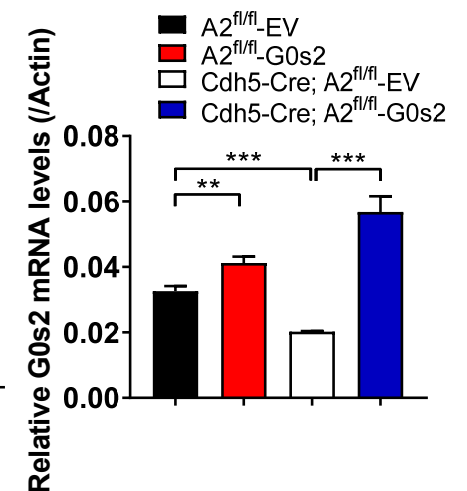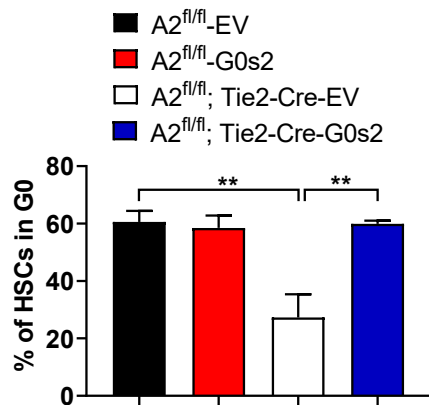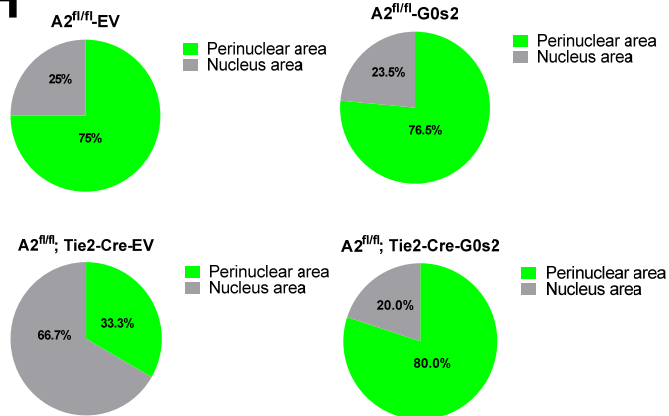**Figure S4, related to Figure 4. ANGPTL2 supports HSC function by sustaining the level of G0S2**. (A-B) Pathway changes in CD34$^+$ human cord blood cells upon treatment with the ANGPTL2 protein as evaluated by RNA-sequencing analyses (A). Potential candidates (*RORA*, *RAB20*, *PIK3R2*, *ISG15 G0S2* and PPARD) for the ANGPTL2-mediated downstream pathway in panel A are shown (B). (C) The changes of potential candidates (*Rora*, *Rab20*, *Pik3r2*, *Isg15*, *G0s2* and *Ppard*) in LT-HSCs from *Cdh5-Cre; Angptl2*$^{fl/fl}$ and *Angptl2*$^{fl/fl}$ mice were determined by RNA-sequencing analysis. LT-HSCs from 6 mice in each group were pooled for the analysis due to the limited number of HSCs from each mouse. (D) Relative mRNA expression of potential candidates (*Rora*, *Rab20*, *Pik3r2*, *Isg15* and *G0s2*) in LT-HSCs purified from *Angptl2*$^{fl/fl}$ and *Tie2-Cre; Angptl2*$^{fl/fl}$ mice as measured by quantitative RT-PCR (n=3). (E) Relative mRNA expression of *G0s2* in total BM cells, Lin$^-$ cells, MPPs, ST-HSCs and LT-HSCs from *Angptl2*$^{fl/fl}$ and *Tie2-Cre; Angptl2*$^{fl/fl}$ mice as measured by quantitative RT-PCR (n=3). (F) *G0s2* levels in BM GFP$^+$ donor cells from *Angptl2*$^{fl/fl}$ and *Cdh5-Cre; Angptl2*$^{fl/fl}$ mice with or without *G0s2* overexpression were determined by quantitative RT-PCR (n=3). (G) The cell cycle status of LT-HSCs from *Angptl2*$^{fl/fl}$ and *Tie2-Cre; Angptl2*$^{fl/fl}$ mice with/without *G0s2* overexpression was determined by staining with Hoechst 33342 and pyronin Y. The percentages of the G0 fraction are shown in G (n=3). (H) Nucleolin localization in LT-HSCs from *Angptl2*$^{fl/fl}$ and *Tie2-Cre; Angptl2*$^{fl/fl}$ mice with/without *G0s2* overexpression was examined by immunofluorescence staining. A total of 15-24 LT-HSCs were analyzed (*$p < 0.05$; **$p < 0.01$; ***$p < 0.001$).
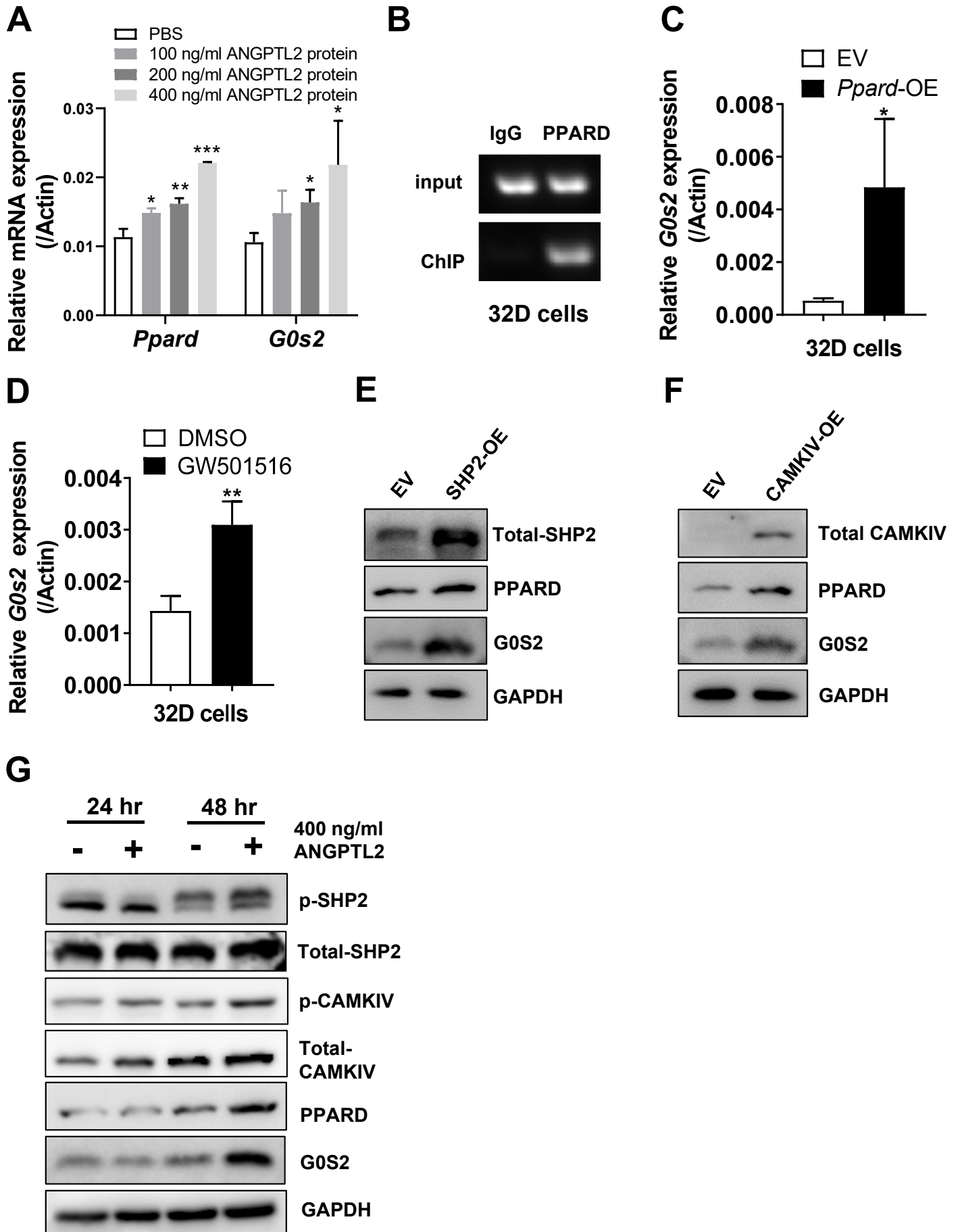
Figure S5

Figure S5, related to Figure 5. ANGPTL2 sustains the level of G0S2 via the PPARD pathway. (A) The *Ppard* and *G0s2* mRNA expression level were determined in LT-HSCs after treatment with different doses of ANGPTL2 protein (100, 200, and 400 ng/mL) for 36 hr by quantitative RT-PCR (n=3). (B) Chromatin immunoprecipitation (ChIP) assays were performed in 32D cells. The *G0s2* promoter regions bound to endogenous PPARD were measured by PCR. (C) The *G0s2* mRNA levels in *Ppard*-overexpressing (Ppard-OE) 32D cells were detected by quantitative RT-PCR (n=3). (D) The *G0s2* mRNA expression levels were measured in 32D cells upon the treatment with PPARD agonist (GW501516) for 24 hr by quantitative RT-PCR (n=3). (E) The protein levels of SHP2, PPARD and G0S2 in SHP2-overexpressing (SHP2-OE) Lin⁻ BM cells were evaluated by immunoblot analysis. (F) The protein levels of CAMKIV, PPARD and G0S2 in CAMKIV-overexpressing (CAMKIV-OE) Lin⁻ BM cells were measured by immunoblot analysis. (G) The protein levels of total-SHP2, p-SHP2, total-CAMKIV, p-CAMKIV, PPARD and G0S2 was determined in Lin⁻ BM cells at 24 and 48 hr after treatment with ANGPTL2 protein by immunoblot analysis.

Supplemental methods

Flow cytometry

BM cells were freshly isolated from 8- to 10-week-old mice and subjected to further flow cytometric analysis. Immunophenotypic $Lin^-Sca-1^+c-Kit^+Flk2^-CD34^-$ LT-HSCs, $Lin^-Sca-1^+c-Kit^+Flk2^-CD34^+$ ST-HSCs, and myeloid and lymphoid progenitor cells ($Lin^-Sca-1^{low}c-Kit^{low}CD16/32^+Flk2^+$ CLPs, $Lin^-Sca-1^-c-Kit^+CD16/32^-CD34^+$ CMPs, $Lin^-Sca-1^-c-Kit^+CD16/32^+CD34^+$ GMPs, $Lin^-Sca-1^-c-Kit^+CD16/32^-CD34^-$ MEPs, and $Lin^-Sca-1^+c-Kit^+Flk2^+CD34^+$ MPPs) were evaluated or FACS-purified by staining with a biotinylated lineage cocktail (anti-CD3, anti-CD5, anti-B220, anti-Mac-1, anti-Gr-1, and anti-Ter119; BD Pharmingen), followed by incubation with streptavidin-PE/Cy5.5, anti-Sca-1-FITC, anti-c-Kit-APC, anti-Flk-2-PE, anti-Flk-2-eFluo450, anti-CD34-PE, and anti-CD16/32-eFluo450 (eBioscience). Differentiated hematopoietic cells, including $Mac1^+F4/80^+$ Macrophages, $CD71^+$ erythroid cells, $B220^+$ B cells, $CD3e^+$ T cells, were stained (all these antibodies were purchased from eBioscience) and sorted for the measurement of *Angptl2* expression as well. For the analysis of the repopulation ability of HSCs, peripheral blood of recipient mice was collected, followed by lysis of red blood cells and staining with anti-CD45.2–FITC, anti-CD45.1–PE, anti-CD3e-APC (for T-lymphoid lineage), anti-B220-PE (for B-lymphoid lineage), anti-Mac-1-APC, or anti-Gr-1-PE monoclonal antibodies (eBioscience; cells costained with anti-Mac-1 and anti-Gr-1 were deemed to be of the myeloid lineage). Cell cycle or apoptotic status was measured in purified $Lin^-Sca-1^+c-Kit^+Flk2^-CD34^-$ LT-HSCs with Hoechst 33342/pyronin Y or anti-annexin V-PE/7-AAD (BD Pharmingen), respectively, as previously described.

Rescue experiment with G0s2 overexpression in HSCs

The XZ201-*G0s2*-GFP-expressing plasmid (or empty vector) and packaging plasmid pCL-ECO (2:1) were transfected into 293T cells. The supernatant was collected at 48-72 hr after transfection. Lin⁻ BM cells isolated from *Angptl2^fl/fl^* and *Cdh5-Cre; Angptl2^fl/fl^* mice were infected by retrovirus with 4 μg/mL polybrene and centrifuged at 800 g for 2 hr, followed by culturing in StemSpan serum-free medium (StemCell Technologies) supplemented with 10 μg/ml heparin (Sigma-Aldrich), 10 ng/ml mouse

SCF (Peprotech), and 20 ng/ml mouse TPO (Peprotech) for 24 hr. Another round of infection was performed before transplantation.

Homing assay

A total of 2×10^7 BM cells were freshly isolated from *Angptl2^{fl/fl}* and *Cdh5-Cre; Angptl2^{fl/fl}* or *Tie2-Cre; Angptl2^{fl/fl}* mice, labeled with CFSE and injected into lethally irradiated recipient mice. The frequencies of CFSE$^+$ cells in the BM, spleen, and liver were determined by flow cytometric analysis 16 hr later. When CFSE$^+$ LSK (Lin$^-$Sca-1$^+$c-Kit$^+$) cells were analyzed, the BM cells were stained with a biotinylated lineage cocktail, followed by incubation with streptavidin-PE/Cy5.5, anti-Sca-1-PE and anti-Kit-APC (eBioscience) before analysis.

Immunofluorescence staining

For immunofluorescence staining of the BM sections, mouse femurs were isolated and fixed in 4% paraformaldehyde at 4°C for 24 hr, followed by decalcification with 0.5 M EDTA (pH 8.0) for another 2 days. The samples were dehydrated in 30% sucrose at room temperature for 30 minutes, embedded in OCT and cryosectioned with a Leica CM3050 cryostat. The BM sections were rehydrated in PBS and permeabilized in 0.5% Triton X-100/PBS solution at room temperature for 15 minutes. The BM sections were then probed with anti-laminin (Abcam), anti-CD150-PE (eBioscience), anti-CD41-APC (Biolegend), anti-CD48-APC (Biolegend) and biotinylated primary antibody cocktail for lineage markers (eBioscience). The BM sections were then washed with PBS and incubated with the appropriate Alexa Fluor-conjugated and streptavidin-APC secondary antibodies at room temperature for 1 hr. Nuclei were counterstained with DAPI before imaging. For the analysis of nucleolin distribution, FACS-purified LT-HSCs were fixed in 4% paraformaldehyde for 10 minutes at room temperature and stained with anti-nucleolin primary antibody (Cell Signaling Technology) at 4°C overnight. Then, the LT-HSCs were incubated with Alexa Fluor 555-conjugated secondary antibody (Thermo Fisher Scientific) for 1 hr, followed by imaging with a Nikon A1 confocal microscope.

Colony assays

A total of 2×10^4 BM cells from *Angptl2^{fl/fl}* and *Cdh5-Cre;Angptl2^{fl/fl}* mice were freshly harvested and seeded in 1.2% methylcellulose IMDM containing 30% fetal bovine serum, 1% bovine serum albumin, 2 mg/mL glutamine, 99 µM β-mercaptoethanol, 50 ng/mL SCF, 20 ng/mL IL-3, 20 ng/mL IL-6, 20 ng/mL erythropoietin (for GEMM, GM and BFU-E assays), 50 ng/mL IL7 (for pre-B assay) or 20 ng/mL erythropoietin (for CFU-E assay). The colonies were counted 7-10 days after culture.

5-FU challenge

Angptl2^{fl/fl} and *Cdh5-Cre; Angptl2^{fl/fl}* or *Tie2-Cre; Angptl2^{fl/fl}* mice (8 mice for each group) were administered intraperitoneally with 5-fluorouracil (5-FU) at a dose of 150 mg/kg/week for 2 weeks. The overall survival was recorded and analyzed using the log-rank test.

Quantitative RT-PCR

First strand cDNA was reversed transcribed using AMV Reverse Transcriptase (TaKaRa). PCRs were performed according to the manufacturer's protocol (Roche). The experiments were conducted with an Applied Biosystems 7900HT system, and the mRNA levels were normalized to the level of the β-actin RNA transcript. The sequences of the primers used are shown in Table S1.

Luciferase reporter assays and chromatin immunoprecipitation analysis

The luciferase reporter vector pGL4.27 containing the *G0s2* promoter was constructed to evaluate the effect of *Ppard* on the transcriptional activation of *G0s2*. The pLVX-Ppard-GFP or negative control vector plasmid along with the pGL4.27-*G0s2* promoter vector were cotransfected into 32D cells, which is myeloblast-like cell line derived from long term cultures of bone marrow cells. Luciferase activities were measured by using a luciferase reporter system (GloMax® Multi Instrument) at 48 hr after transfection. Luciferase measurements were calculated as firefly luciferase units versus Renilla luciferase units. For chromatin immunoprecipitation analysis, 1×10^7 32D cells or Lin^- BM cells were collected, incubated with the anti-PPARD antibody (ab178866, abcam) measured and evaluated the potential binding to *G0s2* promoter by a ChIP Assay Kit (Beyotime Biotechnology). The DNA levels were measured by PCR using primers for G0s2 (Table S1).

Cell culture

Immunophenotypic Lin$^-$Sca-1$^+$c-Kit$^+$Flk2$^-$CD34$^-$ LT-HSCs from WT mice were cultured with StemSpan serum-free medium (StemCell Technologies) supplemented with 10 μg/ml heparin (Sigma-Aldrich), 10 ng/mL mouse SCF (Peprotech), 20 ng/mL mouse TPO (Peprotech) in a U-bottom 96-well plate and treated with different doses of ANGPTL2 protein (100, 200, and 400 ng/mL) for 36 hr, followed by the measurement of mRNA expression levels of *Ppard* and *G0s2* by quantitative RT-PCR. For the treatment of the agonist for PPARD (GW501516), 32D cells and LT-HSCs were incubated with 1μM of GW501516 for 24 hr, followed by the detection of *G0s2* expression by quantitative RT-PCR. For *Ppard* overexpression experiment, The XZ201-Ppard-GFP-expressing plasmid (or empty vector) and packaging plasmid pCL-ECO (2:1) were transfected into 293T cells. The supernatant was collected at 48-72 hr after transfection. 32D cells and Lin$^-$ BM cells isolated from WT mice were infected by retrovirus with 4 μg/mL polybrene and centrifuged at 800 g for 2 hr, followed by culturing for 48 hr. GFP$^+$ 32D cells and Lin$^-$ BM cells were sorted by FACS and subjected to total RNA extraction.

Immunoblot analysis

The XZ201-SHP2-GFP or XZ201-CAMKIV-HA-GFP-expressing plasmid (or empty vector) and packaging plasmid pCL-ECO (2:1) were transfected into 293T cells. The supernatant was collected at 48 hr after transfection. Lin$^-$ BM cells isolated from WT mice were infected by retrovirus with 4 μg/mL polybrene and centrifuged at 800 g for 2 hr, followed by culturing in StemSpan serum-free medium (StemCell Technologies) supplemented with 10 μg/ml heparin (Sigma-Aldrich), 10 ng/ml mouse SCF (Peprotech), and 20 ng/ml mouse TPO (Peprotech) for 48 hr. GFP$^+$ cells were sorted and cell lysates were prepared for the immunoblot analysis. In some cases, Lin$^-$ BM cells were subjected to the treatment with 400 ng/mL of ANGPTL2 protein for 24-48 hr before the analysis. Proteins were separated by electrophoresed on 10% sodium dodecyl sulfate-polyacrylamide gels and transferred onto polyvinylidene difluoride membranes (Millipore). The membranes were incubated with primary antibodies overnight at 4°C, followed by incubation with appropriate horseradish peroxidase conjugated secondary antibodies. The following antibodies were used for the immunoblot analysis: anti-p-SHP2 (D66F10, CST), anti-SHP2 (CY3636, abways),

anti-CAMKIV (sc-55501, Santa Cruz Biotechnology), anti-p-CAMKIV (CY8012, abways), anti-PPARD (ab178866, abcam), anti-G0S2 (A9970, ABclonal), and anti-HA (PTM-5389, PTM BIO).

RNA-Sequencing assay

Human cord blood CD34$^+$ cells treated with or without ANGPTL2 protein were sorted for the extraction of total RNA and subjected to RNA sequencing analyses at Vazyme Biotech Co, Ltd (Shanghai, China). The GEO accession number is GSE169107. Lin$^-$Sca-1$^+$Kit$^+$Flk2$^-$CD34$^-$ immunophenotypic HSCs were purified from *Angptl2$^{fl/fl}$* and *Cdh5-Cre; Angptl2$^{fl/fl}$* mice for the RNA-sequencing analysis at Novogene Co, Ltd (Shanghai, China). The GEO accession number is GSE186454.

Study approval

Human cord blood samples were kindly provided by the Sixth People's Hospital, affiliated to Shanghai Jiao Tong University School of Medicine, Shanghai, China. Written informed consent was obtained from the healthy donor, and all the procedures were approved by the Ethics Committee for Medical Research (IRB) at Shanghai Jiao Tong University School of Medicine.